

Behavior-oriented calculation of the annual coastal bathymetry evolution caused by a reclamation work

ZHENG Jinhai^{1, 2}, HOANG Quoc Xuyen^{1, 2}, ZHANG Chi^{1, 2*}, CHEN Kefeng³, DONG Xiaowei⁴, LEI Gang⁵, WANG Yigang²

¹ State Key Laboratory of Hydrology-Water Resources and Hydraulic Engineering, Hohai University, Nanjing 210098, China

² College of Harbour, Coastal and Offshore Engineering, Hohai University, Nanjing 210098, China

³ Nanjing Hydraulic Research Institute, Nanjing 210024, China

⁴ China Harbour Engineering Company, Beijing 100027, China

⁵ Third Institute of Oceanography, State Oceanic Administration, Xiamen 361005, China

Received 3 December 2016; accepted 10 January 2017

©The Chinese Society of Oceanography and Springer-Verlag Berlin Heidelberg 2017

Abstract

A behavior-oriented formula is improved to calculate the annual coastal bathymetry evolution caused by a reclamation work. This formula is based on a simple hypothesis that, on the time scale of years, the bathymetry evolution is closely related to the change of tidal current field due to the reclamation work. A new coefficient, named the erosion reduction coefficient, is introduced to extend the original formula for applications in calculating bed erosion. A simplified relationship between the annual variation of the siltation/erosion rate and the water depth is introduced to more realistically represent the long-term process of the bathymetry evolution. The improved formula is applied to calculate the bathymetry evolution in 3 a following a reclamation project in the Xiaomiaohong Tidal Channel in Jiangsu coast in China. The results compare well with measurements and those obtained from a process-based numerical model, demonstrating the capability of the improved behavior-oriented formula in reproducing the impact of the reclamation project on the local bathymetry evolution.

Key words: coastal evolution, behavior-oriented formula, reclamation, numerical simulation

Citation: Zheng Jinhai, Hoang Quoc Xuyen, Zhang Chi, Chen Kefeng, Dong Xiaowei, Lei Gang, Wang Yigang. 2017. Behavior-oriented calculation of the annual coastal bathymetry evolution caused by a reclamation work. *Acta Oceanologica Sinica*, 36(11): 86–93, doi: 10.1007/s13131-017-1139-3

1 Introduction

Coastal reclamation works, while very efficient in increasing land resources, can change the natural shoreline and modify hydrodynamics and sediment transport processes. Consequently, the local bathymetry will evolve and re-adapt to the new morphodynamic forcing on a time scale varying from months to years. The evolution of bathymetry following land reclamation is of great concern in coastal engineering since it may affect many aspects, including structure stability, harbor safety, beach protection and local environment.

Over the past decades, various approaches have been developed to quantify the bathymetry evolution caused by extreme natural events (e.g., storms) and human activities (e.g., reclamation, dredging). These approaches may be generally classified into two groups, which are referred to as process-based models (Roelvink et al., 2009; Zhang et al., 2011, 2013, 2014; Zheng et al., 2014) and the behavior-oriented models (Plant et al., 1999; Wang et al., 2001; Splinter et al., 2011). On the basis of numerical solutions to the sophisticated governing equations of the mass and momentum conservation, the process-based models account for

detailed temporal and spatial variations in wave, current and sediment transport. These models are able to reproduce small-scale processes, but often suffer from numerical inaccuracy and instability when dealing with the long-term bathymetry evolution due to the error accumulation effects (Roelvink, 2006). The behavior-oriented models use simple conceptual formulas to estimate the long-term bathymetry evolution, based on the relationships between a few essential parameters dominating the morphodynamic response. These models are simple and much less computational demanding. With adequate site-specific data for model parameterization, these models can give physically reasonable results and have been widely used in engineering practice. The present study will focus on the behavior-oriented models.

Many behavior-oriented models have been developed to study beach profile response, shoreline change, and sandbar migration subject to wave forcing at a time scale of years and a spatial scale of kilometers. The well-known power law equilibrium beach profile formulas were first proposed by Bruun (1954) and Dean (1991), assuming an equilibrium state for constant wave energy dissipation per unit water volume along the profile. The

Foundation item: The National Science Fund for Distinguished Young Scholars of China under contract No. 51425901; the Natural Science Foundation of Jiangsu Province of China under contract No. BK20161509; the Fundamental Research Funds for the Central Universities of China under contract No. 2015B15514; the National Key Technology Research and Development Program of China under contract No. 2012BAB03B01.

*Corresponding author, E-mail: zhangchi@hhu.edu.cn

formulas were further extended to describe the equilibrium beach profile under breaking and non-breaking waves (Larson et al., 1999). Davidson et al. (2013) developed a simple behavior-oriented model for predicting the shoreline change primarily due to cross-shore sediment transport. Their model described the hysteresis effects that future shoreline positions can be strongly dependent on past hydrodynamic conditions and expressed the magnitude of the shoreline change as a function of the time-varying disequilibrium degree. The behavior-oriented models have also been developed for the sandbar migration and may predict the temporal variations in the alongshore-averaged sandbar position (Plant et al., 1999; Pape et al., 2010) and the alongshore variability of a sandbar (Splinter et al., 2011). These models are mainly based on the breaking-point hypothesis that, in the variable wave climate, the sandbar migrates towards a breaking-point-dependent equilibrium position at a speed related to both response time and the instantaneous distance from the equilibrium position. The sandbar migration is dominated by wave non-linearity and undertow (Zhang et al., 2017, 2014; Dong et al., 2014). It is noted that the above models have been developed and verified under the following conditions: (1) the coast is composed of sandy sediment and has pronounced morphological features (e.g., sandbar, berm); (2) the coastal evolution is wave-dominated; and (3) effects of human activities are not significant. Therefore, they may not be suitable for application to the tide-dominated muddy coastal evolution affected by engineering projects, which is mostly the case along China's coastline.

Luo (1987) and Liu and Zhang (1992) developed behavior-oriented formulas to calculate the sediment siltation rate in navigation channels and harbor basins due to dredging works on muddy coasts. Wang et al. (2001) derived a simple behavior-oriented formula to calculate the sediment siltation rate around the reclamation area on muddy coasts. This formula has been successfully applied to calculate the bed siltation for a period of 3 a after a reclamation project in the Hangzhou Bay in China (Wang et al., 2001). The aforementioned approaches are based on a similar hypothesis, i.e., engineering-induced change in the local sediment carrying capacity of tidal current leads to suspended sediment settling and bed siltation. The change in the tidal current field may be due to the changes in water depth and shoreline as a result of dredging or reclamation works. These formulas are suitable for local bed siltation near the engineering projects on tide-dominated muddy coasts, where most sediments are transported as suspended load. However, most of these formulas focus on predicting sediment siltation, and less attention has been paid to bed erosion. The verification of these formulas for both sediment siltation and erosion in real engineering projects is still rare since the field data recording the long-term bathymetry change induced by engineering project is often unavailable.

In this study, we improve the behavior-oriented formula originally introduced in Wang et al. (2001) for the bathymetry evolution caused by a reclamation project. The improved formula has the advantage of being able to calculate both bed siltation and erosion. A simplified approach is further introduced to save computational time for a long-term prediction. The improved formula will be tested against the bathymetry change around a reclamation project measured for 3 a in the Xiaomiaohong Tidal Channel of Jiangsu Province, China.

2 Behavior-oriented formula

2.1 Revisiting the original formula

Wang et al. (2001) developed a simple behavior-oriented for-

mula to calculate the suspended sediment siltation rate for muddy coasts with reclamation work, expressed as

$$P = n\Delta P = \frac{\alpha n S_{s,1} H}{\gamma_c} \left(1 - \frac{S_{s,2}}{S_{s,1}} \right), \quad (1)$$

where P is the annual siltation rate; n is the number of tidal cycles per year; ΔP is the siltation rate for a representative tidal cycle; γ_c is the dry sediment bulk density; α is the sediment settling probability; H is the average water depth; and $S_{s,1}$ and $S_{s,2}$ are the sediment carrying capacities before and after the reclamation project, respectively. The sediment carrying capacity can be calculated by

$$S_s = k \left(\frac{u^2}{gH} \right)^m, \quad (2)$$

where u is the average tidal current velocity; g is the gravity acceleration; and k and m are site-dependent coefficients to be calibrated against local field data.

Combining Eq. (1) and Eq. (2) gives

$$P = n\Delta P = \frac{\alpha n S_{s,1} H}{\gamma_c} \left[1 - \left(\frac{u_2}{u_1} \right)^{2m} \right], \quad (3)$$

where u_1 and u_2 are the average tidal current velocities before and after the reclamation project, which may be provided by a two-dimensional tidal current numerical model. Equation (3) is based on a physical consideration, i.e., the local bed siltation is related to the excess sediment settling associated with the reduction of sediment carrying capacity for a decreasing tidal current velocity (e.g., $u_2/u_1 < 1$). This is often the case close to the coastal reclamation structures.

However, the two shortcomings of Eq. (3) should be noted. First, its applicability for calculating the bed erosion has not been addressed. Although Eq. (3) gives negative values of the annual siltation rate when the ratio of the average tidal current velocities after to before the reclamation is greater than 1 ($u_2/u_1 > 1$) (i.e., the increasing sediment carrying capacity leads to bed erosion), whether these results are physically realistic is still unclear. Therefore, Eq. (3) was commonly not used to calculate the bed erosion and the obtained negative values of the annual siltation rate were simply set to be 0 in the previous studies. Second, for every year the tidal current numerical model should be rerun with the updated bathymetry to obtain the annual siltation rate for the following year. This requires additional computational efforts when dealing with a long-term bathymetry evolution in engineering practice.

2.2 Improved formula in the present study

At first, we discuss the applicability of this type of formula to calculate the bed erosion. From a physical perspective of point, increase in the sediment carrying capacity (i.e., $u_2/u_1 > 1$) will indeed lead to the increase in the sediment concentration within the water column and cause the bed erosion ($P < 0$). This physical hypothesis is similar to the case of the bed siltation. However, the quantitative relationship between the annual siltation rate and the ratio of the average tidal current velocities after to before the reclamation (u_2/u_1) may not be identical. It is noted that the bed erosion only occurs when the instantaneous current velocity

exceeds the incipient velocity of bed sediment. Although the time-averaged tidal current velocity after the reclamation project is larger than that prior to the project, the instantaneous current velocity may be still lower than the incipient velocity and unable to erode the bed sediment during part of a tidal cycle. This will lead to shorter effective time for the bed erosion and so the real erosion rate will be smaller than that directly calculated by Eq. (3). Owing to the complex mechanism of coastal sediment transport, it is difficult to derive a definite theoretical expression for this process. The exact incipient velocities at different locations are also difficult to determine and variable with time. On the other hand, the average tidal current velocity in Eq. (3) is a time-averaged quantity and it is therefore not straightforward to compare these two velocities in such a simplified formula. In practice, we may improve the formula by introducing a simple erosion reduction coefficient to describe the reduction of the erosion intensity due to the restriction of the incipient velocity. The improved formula becomes more suitable and practical for the calculation of both bed siltation and erosion:

$$P = n\Delta P = \beta \frac{\alpha n S_{c,1} H}{\gamma_c} \left[1 - \left(\frac{u_2}{u_1} \right)^{2m} \right], \quad (4)$$

where β is the erosion reduction coefficient ($\beta = 1.0$ for $u_2/u_1 \leq 1$ and $\beta < 1$ for $u_2/u_1 > 1$).

The erosion reduction coefficient (β) is a new parameter and little guidance is available to determine its value. As a preliminary approximation, the erosion reduction coefficient (0.8) is used for the present case which produces a model prediction in good agreement with field data. It is noted that the exact value of the erosion reduction coefficient could be affected by various factors. For example, it should be larger for a larger tidal range (i.e., larger current velocity) and smaller water depth and bed sediment size (i.e., smaller incipient velocity). Future research efforts are required to establish a more comprehensive relationship between the erosion reduction coefficient and various hydrodynamic and sediment parameters based on more field data.

The second attempt is to reduce the computational cost involved in the application of this behavior-oriented formula. This is achieved using a simplified relationship between the annually variation in siltation/erosion rates and that in the water depth:

$$\frac{P_{i+1}}{P_i} = \begin{cases} \frac{H_i}{H_{i-1}} & P_i \geq 0 \\ \frac{H_{i-1}}{H_i} & P_i < 0 \end{cases} \quad i = 1, 2, 3, \dots, \quad (5)$$

where P_i and H_i are respectively the siltation/erosion rate and the average water depth in the i th year after the reclamation project. Note that the ratio of the siltation rates in i th+1 year to i th one after the reclamation project (P_{i+1}/P_i) is always less than 1. The positive and negative siltation rate in the i th year (P_i) indicate siltation and erosion, respectively. Equation (5) is based on the following physical consideration. The continuous decrease in the water depth due to the bed siltation implies an increasing current velocity and sediment carrying capacity as well as a decreasing flood duration, leading to a suppressed siltation rate. On the other hand, the continuous increase in the water depth due to the bed erosion implies a decreasing current velocity and sediment carrying capacity together with an increasing flood duration, resulting in a reduced erosion rate. Therefore, after the re-

clamation project, the annual siltation/erosion rate will gradually decrease with time due to the bathymetry re-adaptation to the new hydrodynamic forcing. In other words, the bathymetry evolution slows down as it becomes closer to the steady state which is mainly controlled by the water depth variation. It is thus hypothesized that the decreasing in the siltation/erosion rate between two successive years is approximately proportional to the change in the water depth between the previous two years. Therefore, Eq. (5) describes a physically reasonable process of the bathymetry evolution for multiple years, but it only requires running the tidal current numerical model once for the first year. This effectively save computational cost in practice, especially for the long-term calculations.

3 Application

In this section, the improved behavior-oriented formula is used to calculate the morphological change of the Xiaomiaohong Tidal Channel on the Jiangsu coast of China from 2003 to 2006, following the construction of a land reclamation project on the south bank in 2003. The calculated results will be compared with the measured data.

3.1 Field observation

The Xiaomiaohong Tidal Channel is located at the southern part of a large-scale radial sand ridge system along the Jiangsu coast (Fig. 1). The 38 km long channel is parallel to the shoreline with a distance of 3.5–6.0 km. Two shallow shoals, namely Hengsha Shoal and Wulong Shoal, exist in the channel entrance, dividing the Xiaomiaohong Channel into the North Channel, the Middle Channel and the South Channel. In the Middle Channel and the South Channel, there are two deep troughs with a water depth greater than 10 m. The median suspended sediment size in the channel is 0.007 mm. According to Chen et al. (2012) and Zhang et al. (2013), the bathymetry evolution in the Xiaomiaohong Tidal Channel is dominated by the regular semidiurnal tide and the rectilinear tidal current.

A reclamation project was constructed in 2003 on the south bank of the Xiaomiaohong Tidal Channel, as shown in Fig. 1. The reclamation project resulted in considerable change in the channel bathymetry. Figure 2 shows the bathymetries measured respectively in 2003 and 2006. Figure 3 shows the bathymetry change measured during 3 a after the project. It is observed that the overall pattern of the channel remains unchanged, but obvious siltation or erosion can be found at the end of channel and around the project area. As discussed by Chen et al. (2012) and Zhang et al. (2013), the impacts of the reclamation project are mainly concentrated near the project area. The bed siltation occurred on both east and west sides of the project area, and the erosion is found to deepen the trough at the northwest corner. The siltation on the east side is larger than the west side.

Considering that the behavior-oriented formulas of this type have not been extensively tested against field data, the measured bathymetries of the Xiaomiaohong Tidal Channel before and after the reclamation project are thus valuable. The present study will mainly focus on the bathymetry change around the reclamation area (i.e., the morphological response to the engineering project) which is particularly concerned in engineering works.

3.2 Formula setup

In Eq. (4), several parameters are needed to be determined. Sedimentation probability α is related to the grain size, the current velocity and other factors. When the median grain diameter is less than 0.03 mm, the average floc settling velocity is around

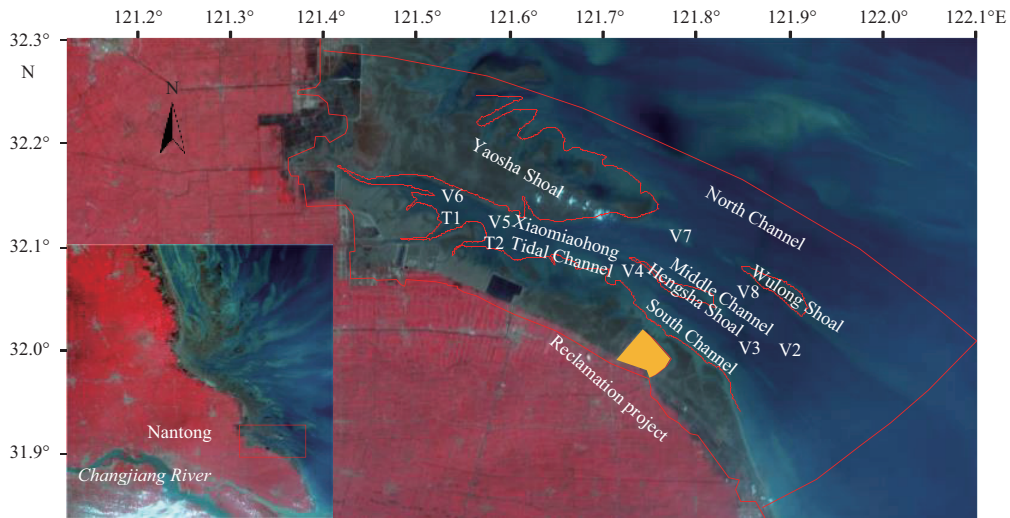


Fig. 1. Location of the Xiaomiaohong Tidal Channel and the reclamation project.

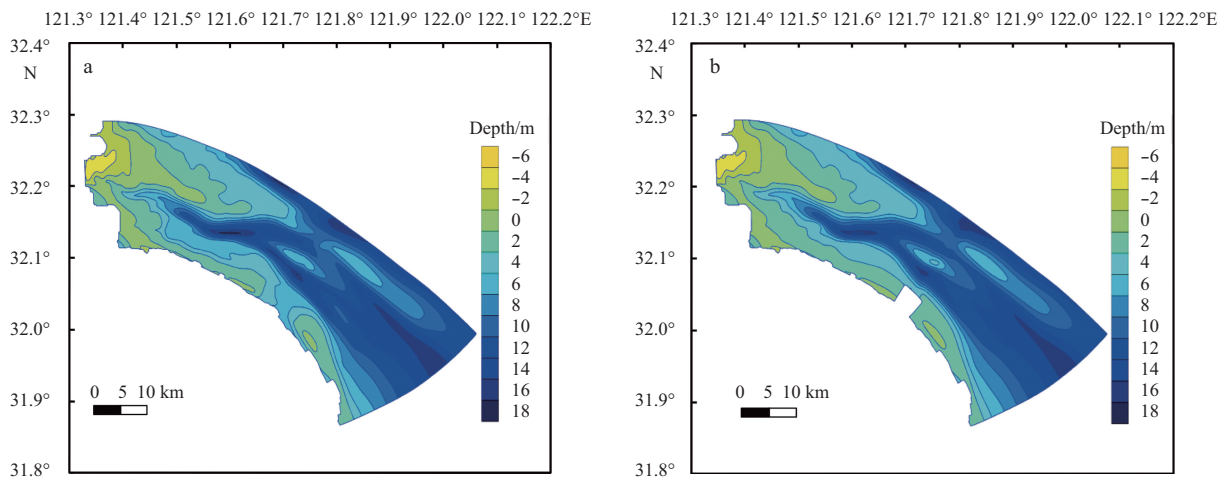


Fig. 2. Measured bathymetries of the Xiaomiaohong Tidal Channel in 2003 (a) and 2006 (b).

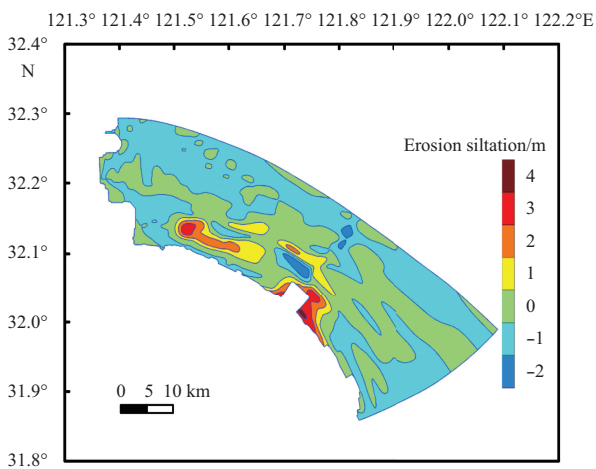


Fig. 3. Measured bathymetry change of the Xiaomiaohong Tidal Channel from 2003 to 2006.

0.4 mm/s and the average sedimentation probability is 0.67, according to Luo (1987). The tide in this region is regular semi-

urnal tide. There are two high water levels and two low water levels in every lunar day and the tidal cycle is 12 h and 25 min. Therefore, the tidal cycle number N in a year is 705.

The sediment carrying capacity S is determined through the regression analysis of the measured tidal current velocity and the sediment concentration at seven locations in the middle and south channels during 26 March and 27 March in 2009. It is found that the current velocity and the sediment concentration are well correlated. The regression curve of the sediment carrying capacity obtained by a least square fitting method is shown in Fig. 4. The sediment carrying capacity in the Xiaomiaohong Tidal Channel can be reasonably represented by the following equation:

$$S = 1.046 \left(\frac{u^2}{gH} \right)^{0.132}. \quad (6)$$

The average tidal current velocities before and after the project are important as they control the patterns of siltation and erosion in the whole domain. In the present study, the Delft3D model (Lesser et al., 2004) is used to obtain the tidal current field

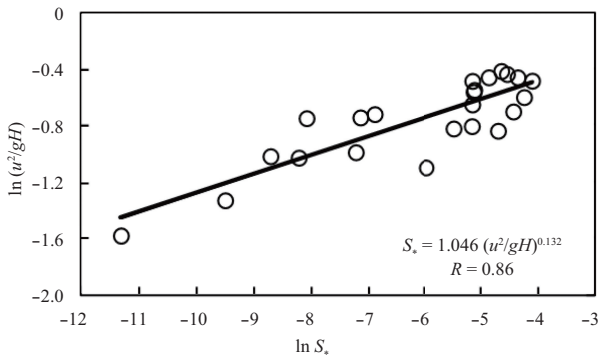


Fig. 4. Regression analysis of sediment carrying capacity.

and hence the velocities. The computational domain is 65 km long in x -direction and 45 km long in y -direction covering the whole tidal channel, which is discretized using an orthogonal curvilinear mesh with 15 934 grid cells (Fig. 5). The grid size varies from 100 to 400 m with the locally refined mesh created close to the project area. The computational time step is 30 s. Open boundary conditions are imposed with the water level forecasted by NAOTIDE (Matsumoto et al., 1995). During the simulation, the horizontal eddy viscosity coefficient is 1.0 m²/s, and Manning coefficient is set to be 1/80.

The model is validated by the measured tidal levels at two locations (T1 and T2) and the measured tidal current velocities at seven locations (V2–V8) in the Xiaomiaohong Tidal Channel for 26 March to 27 March in 2009, corresponding to the spring tide.

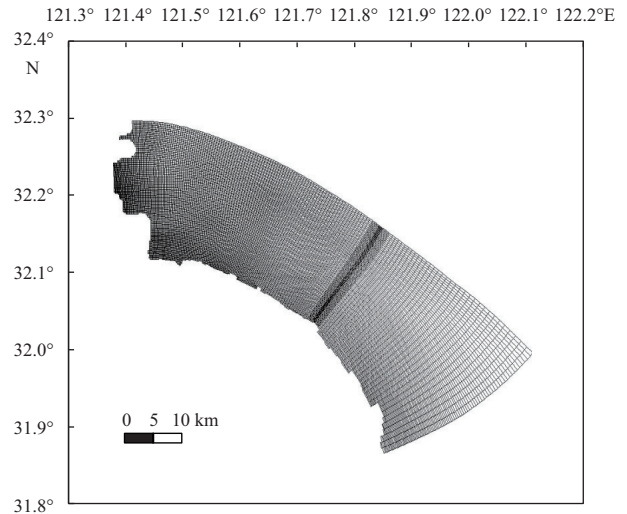


Fig. 5. Computational model domain.

The locations of the gauge points are shown in Fig. 1. Figures 6–8 show the comparison between the model results and the measured data, in terms of the water level, the current velocity and the current direction, where the measured data and the modeled results are respectively plotted as symbols and lines. Achieving satisfactory model-data agreements, the tidal current velocities before and after the project can be simulated and input into Eq. (4) to investigate the impact of the reclamation project.

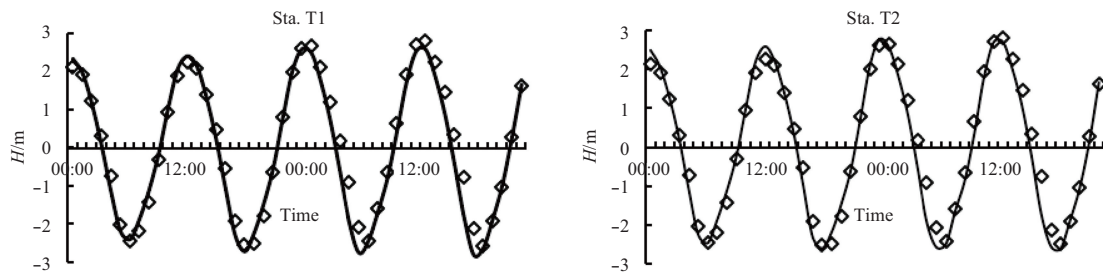


Fig. 6. Comparisons of water depths at Stas T1 and T2.

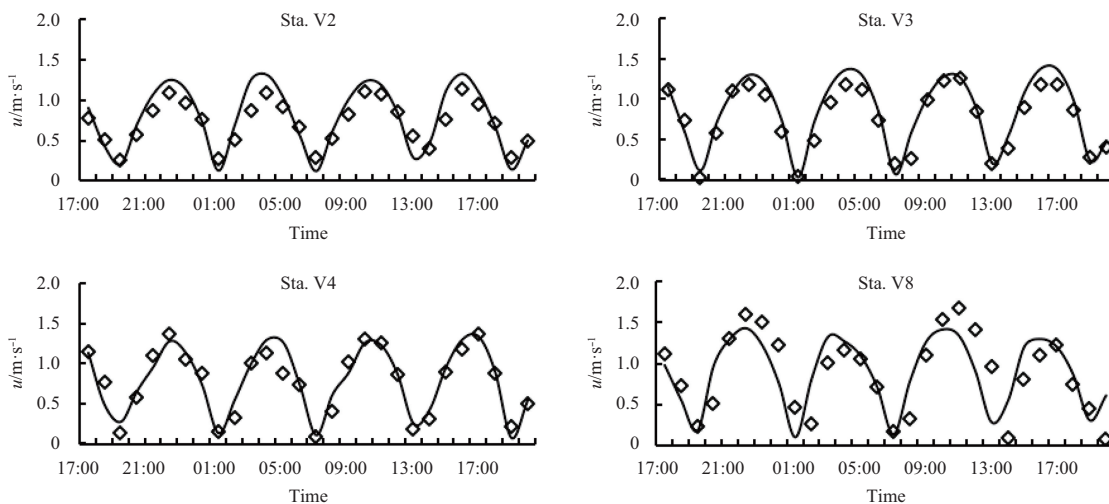


Fig. 7. Comparisons of current velocity at four locations.

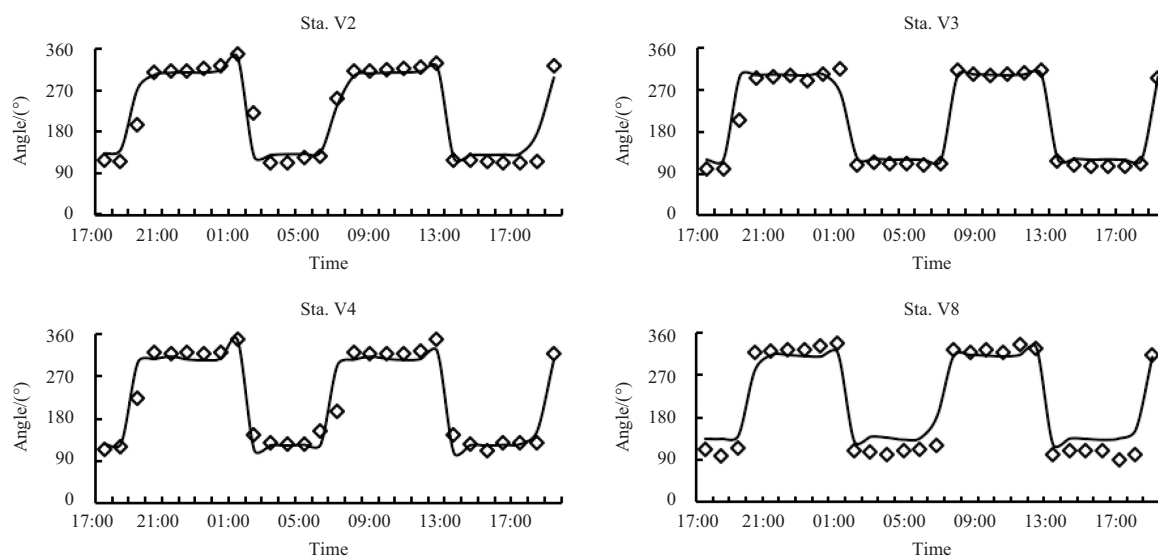


Fig. 8. Comparisons of current direction at four locations.

3.3 Calculated results

Figure 9 shows the distribution of the erosion and siltation thickness predicted by the improved formula. Significant siltation can be observed on both sides of the project with a maximum siltation thickness of 2 m. The siltation thickness and area are larger on the east side than west side. There is a large area of erosion at the northwest corner of the project area, in which the erosion thickness reaches the maximum value of around 2 m in the vicinity of the project and decreases as the distance increases. This is consistent with the field observation as shown in Fig. 3. The siltation on both sides of the project area is due to the blocking effects of the project on the tidal current and sediment transport parallel to the shoreline, which decreases the local current velocity and leads to a decrease of the sediment carrying capacity. The erosion at the northwest corner is resulted from the combined effects of the decrease in the cross-sectional area of waterway, the local increase in the tidal current velocity and the singularity of the new shoreline. In general, the main features of bathymetry changes around the project area are correctly captured by the improved formula, demonstrating that this behavior-oriented formula can reasonably describe the local morphological response to the reclamation project. However, there is a quantitative difference between Fig. 3 and Fig. 9. It is noted that the present formula is only suitable for the bathymetry change purely due to the reclamation project, but is not established to account for the natural bathymetry evolution that occurs in the whole tidal channel. Therefore, the quantitative difference between calculation and observation may be due to the natural bathymetry evolution.

3.4 Discussion

To further investigate the accuracy of the proposed formula, it is of interest to isolate the bathymetry change caused only by the reclamation project from the total change. For this purpose, an assumption was made that the total bathymetry change is a linear superposition of the changes caused by the project and the natural waterway evolution. In other words, the bathymetry changes purely caused by the project can be obtained by removing the natural evolution from the total bathymetry change. In this section, the latter two morphological processes are simu-

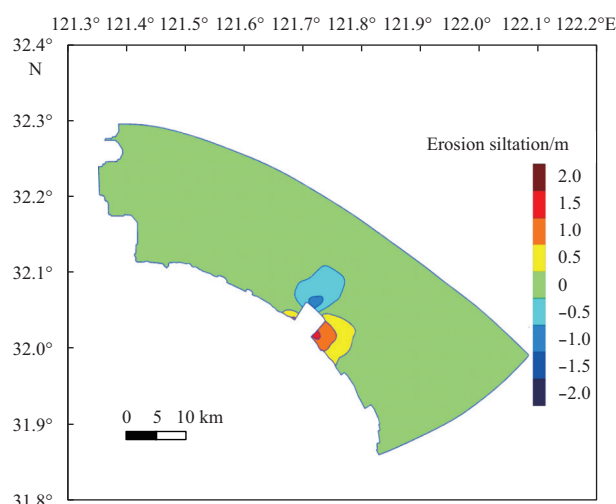


Fig. 9. Reclamation-induced bathymetry change calculated by the improved formula.

lated by the Delft3D model.

The tidal level series at the offshore boundaries from 1 January 2003 to 1 January 2006 is predicted by the NAOTIDE and used as the offshore boundary conditions for the morphological calculation. Figure 10 shows the total bathymetry change simulated by the Delft3D model. Comparing Figs 3 and 10, it is noted that the simulated overall erosion/siltation patterns are similar to the observation. Siltation of 2–3 m thickness occurs around the project area. The closer to the project the larger the siltation intensity is. The siltation area on the east side of the project is larger than that on the west side. Between the northwest corner of the project and the South Channel, there is an obvious erosion. Between the main channel and the shore, there exists a siltation region along the channel direction with a ribbon shape, consistent with the observation. In the large-scale area east of the project region, erosion occurs in both simulation and observation. The model correctly reproduces the two peak erosion regions close to the north and east open boundaries, respectively.

In order to quantitatively evaluate the accuracy of the model

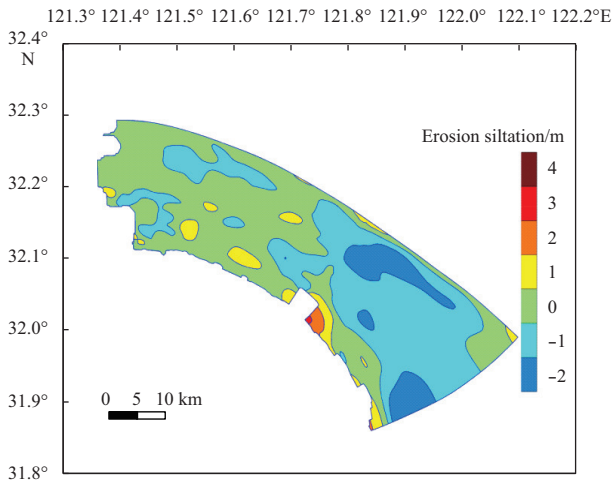


Fig. 10. Total bathymetry change simulated by the Delft3D model.

result, the Brier Skill Score (BSS) is introduced, which has been widely applied in assessing coastal morphology evolution modeling (van Rijn et al., 2003). The BSS compares the mean square difference between the prediction and the observation with the mean square difference between the baseline prediction and observation. The BSS values are respectively 0.75 and 0.90 for the whole computational domain and for the local region within 5 km distance from the project (Table 1). According to van Rijn et al. (2003), this indicates that the model predictability is satisfactory for the whole domain and is excellent for the local area close to the project. This also implies that the project influence is quantitatively well reproduced by the model.

Table 1. Qualification of the Delft3D model performance

Area	BSS	Qualification
The whole domain	0.75	good
The local region within 5 km distance from the project	0.90	excellent

The natural morphology evolution (Fig. 11) can be obtained by rerunning the model starting from the natural bathymetry, without considering the project. The reclamation-induced bathymetry evolution is then obtained by removing the natural evolution from the total evolution, as shown in Fig. 12. It can be seen from Fig. 11 that the natural bathymetry evolution has an important contribution to the total evolution in this region. This is also the case around the project area. Therefore, the quantitative difference between the formula prediction and the observation in Section 3.3 is indeed due to the natural bathymetry evolution. Comparing Figs 12 and 9, it is found that the results produced by the improved behavior-oriented formula are consistent with the process-based model in both erosion/siltation intensities and distribution patterns. This further confirms that the improved formula can well predict the coastal morphology evolution caused by the reclamation project with a reasonable accuracy. It is also noted that, when a process-based model is used to assess the engineering-induced bathymetry change, it is necessary to remove the contribution of the natural evolution from the results.

4 Conclusions

An improved behavior-oriented formula to calculate the an-

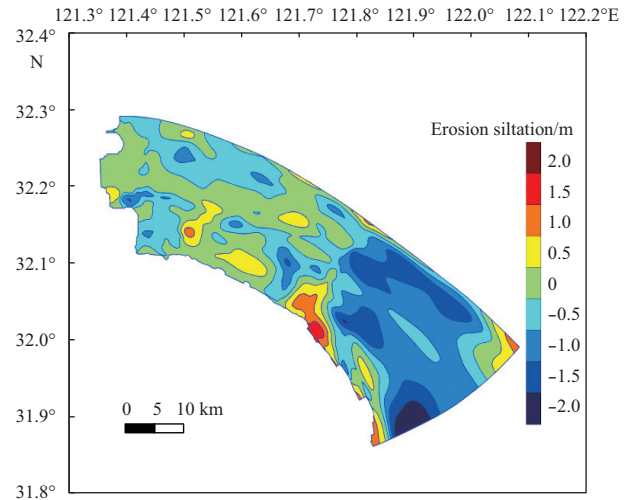


Fig. 11. Natural bathymetry change simulated by the Delft3D model excluding the effects of the reclamation project.

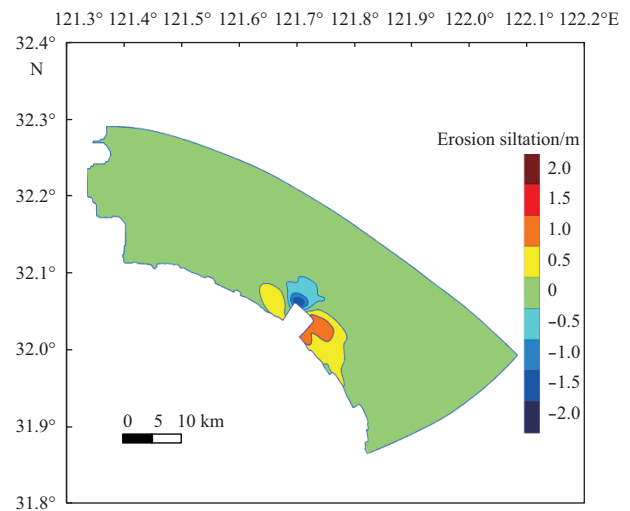


Fig. 12. Reclamation-induced bathymetry change simulated by the Delft3D model.

nual coastal bathymetry evolution caused by the reclamation work is developed based on the original formula of Wang et al. (2001). Compared with the original formula, an erosion reduction coefficient is introduced to extend the applicability of the formula to calculating the bed erosion, and a simplified relationship between the annually variations of the siltation/erosion rate and the water depth is introduced to save computational time for long-term calculation. The improved formula is applied to calculate the 3a bathymetry evolution around a reclamation project in the Xiaomiaohong Tidal Channel in Jiangsu coast in China. The formula prediction is compared with both the measured data and the numerical results provided by the Delft3D model. It is shown that the impact of the reclamation project on the local bathymetry evolution can be well reproduced by the improved behavior-oriented formula.

Owing to the lack of data, this study is restricted to the case of the Xiaomiaohong Tidal Channel. It is noted that more comprehensive validation at different places is important to examine or improve the general effectiveness of the proposed formula. Collecting more field data and conducting more case studies will be

the focus of the future work.

Nevertheless, this study demonstrates a few important issues that have not been clarified so far. While the previous studies focused on the behavior-oriented calculation of sediment siltation, the present study shows that the formulas of this type also have the potential to calculate the bed erosion by introducing an erosion reduction coefficient. It is further found that such a simple empirical formula can provide equally reliable predictions as a process-based numerical model does in terms of the bathymetry change caused by the reclamation work. Moreover, this study indicates that how the total bathymetry evolution may be effectively separated into the natural contribution and the engineering project-induced contribution. The above points could be useful for assessing morphological impacts of the reclamation projects in coastal engineering practice.

References

- Bruun P. 1954. Coast Erosion and the Development of Beach Profiles. Technical Memorandum 44. Washington, DC: US Beach Erosion Board
- Chen Kefeng, Lu Peidong, Yu Guohua. 2012. Hydrodynamic mechanism of morphology revolution of the Xiaomiaohong Tidal Channel in radial sand ridges, Jiangsu province. *Acta Scientiarum Naturalium Universitatis Sunyatseni* (in Chinese), 51(2): 101–106
- Davidson M A, Splinter K D, Turner I L. 2013. A simple equilibrium model for predicting shoreline change. *Coastal Engineering*, 73: 191–202
- Dean R G. 1991. Equilibrium beach profiles: characteristics and applications. *Journal of Coastal Research*, 7(1): 53–84
- Dong Guohai, Chen Hongzhou, Ma Yuxiang. 2014. Parameterization of nonlinear shallow water waves over sloping bottoms. *Coastal Engineering*, 94: 23–32
- Larson M, Kraus N C, Wise R A. 1999. Equilibrium beach profiles under breaking and non-breaking waves. *Coastal Engineering*, 36(1): 59–85
- Lesser G R, Roelvink J A, van Kester J A T M, et al. 2004. Development and validation of a three-dimensional morphological model. *Coastal Engineering*, 51(8–9): 883–915
- Liu Jiaju, Zhang Jingchao. 1992. Siltation prediction for navigation channels and harbour basins on muddy beach. *China Ocean Engineering*, 6(2): 157–172
- Luo Zhaosen. 1987. Computation of siltation in dredged channels in estuaries. *Journal of Sediment Research* (in Chinese), (2): 13–20
- Matsumoto K, Ooe M, Sato T, et al. 1995. Ocean tide model obtained from TOPEX/POSEIDON altimetry data. *Journal of Geophysical Research: Oceans*, 100(C12): 25319–25330
- Pape L, Plant N G, Ruessink B G. 2010. On cross-shore migration and equilibrium states of nearshore sandbars. *Journal of Geophysical Research: Earth Surface*, 115(F3): F03008
- Plant N G, Holman R A, Freilich M H, et al. 1999. A simple model for interannual sandbar behavior. *Journal of Geophysical Research: Oceans*, 104(C7): 15755–15776
- Roelvink D, Reniers A, van Dongeren A, et al. 2009. Modelling storm impacts on beaches, dunes and barrier islands. *Coastal Engineering*, 56(11–12): 1133–1152
- Roelvink J A. 2006. Coastal morphodynamic evolution techniques. *Coastal Engineering*, 53(2–3): 277–287
- Splinter K D, Holman R A, Plant N G. 2011. A behavior-oriented dynamic model for sandbar migration and 2DH evolution. *Journal of Geophysical Research: Oceans*, 116(C1): C01020
- van Rijn L C, Walstra D J R, Grasmeyer B, et al. 2003. The predictability of cross-shore bed evolution of sandy beaches at the time scale of storms and seasons using process-based profile models. *Coastal Engineering*, 47(3): 295–327
- Wang Yigang, Li Xi, Lin Xiang. 2001. Analysis on suspended sediment deposition rate for muddy coast of reclaimed land. *China Ocean Engineering*, 15(1): 147–152
- Zhang Chi, Zhang Qingyang, Zheng Jinhai. 2017. Parameterization of nearshore wave front slope. *Coastal Engineering*, 127: 80–87
- Zhang Chi, Zheng Jinhai, Dong Xiaowei, et al. 2013. Morphodynamic response of Xiaomiaohong Tidal Channel to a coastal reclamation project in Jiangsu Coast, China. *Journal of Coastal Research*, 65: 630–635
- Zhang Chi, Zheng Jinhai, Wang Yigang, et al. 2011. A process-based model for sediment transport under various wave and current conditions. *International Journal of Sediment Research*, 26(4): 498–512
- Zhang Chi, Zheng Jinhai, Zhang Jisheng. 2014. Predictability of wave-induced net sediment transport using the conventional 1DV RANS diffusion model. *Geo-Marine Letters*, 34(4): 353–364
- Zheng Jinhai, Zhang Chi, Demirbilek Z, et al. 2014. Numerical study of sandbar migration under wave-undertow interaction. *Journal of Waterway, Port, Coastal, and Ocean Engineering*, 140(2): 146–159